REVISTAMATÉRIA V.30
ISSN 1517-7076 artigos e20250611, 2025

Enhancing mechanical properties of Al-SiC metal matrix composites: A study on reinforcement effects and fracture behaviour using acoustic emissions technique

Chandra Sekar Kanthaswamy[1], Sasikumar Thangaswamy[1], Sunesh Narayanaperumal[2], Arunprasath Kanagaraj[2]

[1]Rohini College of Engineering & Technology, Department of Mechanical Engineering. 629401, Anjugramam, Tamil Nadu, India.

[2]Alliance University, Alliance School of Applied Engineering, Sophisticated Testing and Instrumentation Centre, Department of Mechanical Engineering. 562106, Bengaluru, Karnataka, India.

e-mail: kchandrasekarmech1@gmail.com, sasikumar.t2000@gmail.com, nsunesh16@gmail.com, aruncmr12@gmail.com

ABSTRACT

The structural and mechanical properties of Aluminium-Silicon Carbide (Al-SiC) metal matrix composites (MMCs) made by stir casting are investigated when SiC is added at a range from 0% to 10% by weight. The work examines the primary mechanical properties, including tensile strength, flexural strength, impact strength, hardness, and low-velocity impact resistance, as well as microstructure and acoustic emission analyses. The fact that increasing SiC makes the material stronger and tougher is evident in the results, with tensile strength increasing to 349.57 MPa (a 24.5% rise over pure Al), flexural strength reaching 240.85 MPa (a 108.8% increase over pure Al), and hardness reaching 101.25 BHN. With an increased proportion of SiC in the mixture, the ductility and ability to change shape decrease. The addition of SiC results in a steady increase in impact strength, with the highest level of 53.68 kJ/m^2 achieved at a 10% concentration, demonstrating the material's crack resistance. According to the research, Al-SiC MMCs exhibit the best mechanical properties for aerospace and automotive applications when the reinforcement levels are just right. Hybrid reinforcements or small SiC fibers may be examined in future work to reduce brittleness while retaining the best features.

Keywords: Metal matrix composites; Aluminium-silicon carbide; Stir casting; Acoustic emission.

1. INTRODUCTION

A composite material consists of combining two or more materials, which have differences in how they're made and what they look like in composition. The discrete component, or reinforcement, focuses on building the hypothesis in the example. The continuous part of the reaction is referred to as the matrix [1, 2].

One type of advanced material is known as a metal matrix composite, where metal and common ceramic particles are brought together. The properties of the MMC are more advantageous than those of the base metal [3]. Improved thermal conductivity, resistance to being abraded, tribology, ability to resist creep, solid shape, and exceptional stiffness are the mentioned properties. Just as other composites, aluminium matrix composites are a group of materials that can be tailored in stiffness, strength, density, thermal, and electrical properties [4, 5].

Al-SiC MMCs are produced through Powder metallurgy, melt infiltration and stir methods. Some places also use casting and Squeeze casting. Among the various techniques, stir casting is most commonly chosen due to its unique features [6]. The simplicity of this type of production allows it to produce a wide range of components, and productivity and size do not limit its targets. In stir casting, the primary challenge is that reinforcing elements tend to agglomerate during solidification, resulting in loss of mechanical properties [7, 8]. A review of related literature indicates that reinforcement is distributed as follows. The motion of particles can be controlled by changing the stirrer speed, volume fraction and the shape of the stirrer blades. Clumping of reinforcing materials during solidification is considered the primary limitation of stir casting. Negatively affects the mechanical

Corresponding Author: Chandra Sekar Kanthaswamy Received on 11/07/2025 Accepted on 28/10/2025

DOI: https://doi.org/10.1590/1517-7076-RMAT-2025-0611

performance of materials. By examining studies in this area, we have gained insight into how reinforcement is distributed [9, 10]. Processing particulars, including stirrer speed and the geometry of its blades, decide how well particles will be mixed, etc.

Additionally, the challenge for people in the foundry is that the molten metal cools rapidly during melt stir casting. The metal gets filled into the mould. The rapid reduction in temperature of molten metal inside the composite leads to the formation of hollow areas. The stir-cast MMCs' properties are impacted by the rate at which their metal solidifies [11, 12]. Several experts have done real-time experiments to understand solidification phenomena and examine the Solidification behaviour for Al SiC MMC, which is influenced by several processing factors. A team led by Behra carried out the study. I found during fluidity tests that there is a decrease in fluidity when the reinforcement percentage increases. The combination of Al_4C_3 at the boundary also leads to a local hardening of the metal matrix. It can be seen that Particle reinforcement can change the nature of the final composite microstructure. Because of this, we have to contend with the mechanical performance of composites [13, 14].

INEGBENEBOR *et al.* [15] proved that when silicon carbide (SiC) was dispersed using stir casting in aluminium, the properties of the composites improved. With 2.5%, 5.0%, 7.5% and 10% SiC, both Young's modulus and hardness of the sample were higher than those of the base metal. When the volume fraction was 7.5%, the 1200-grit SiC was stronger, with a modulus of 1517.6 MPa, and more resistant, with a hardness of 26.1 Hv. Both sizes of SiC grit reduced the electrical conductivity compared to the unimproved aluminium.

The wear characteristics, strength, compactness, and hardness of stir-cast aluminium–silicon carbide (Al–SiC) metal matrix composites are systematically evaluated. Among the 0%, 2.5% and 5% SiC specimens, wear loss was largest at both extremes. Different loads and sliding distances affected the write rate and specific wear rate, with the 0% sample exhibiting the least wear. With a higher percentage of SiC, the hardness and strength of the sintered blocks rose, and the maximum BHN was found to be 254 at 5% SiC [16, 17].

SOUNDARARAJAN *et al.* [18] focuses on the fabrication and analysis of A356-20wt%SiC metal matrix composites, exploring how different processing methods, such as mechanical stirring and ultra-sonic assisted cavitation, impact their physical and mechanical properties. The research highlights improvements in densification, hardness, and tensile strength when utilizing ultrasonication, explaining these enhancements through observed microstructural evolutions that prevent particle clustering [19, 20].

SATHISHKUMAR *et al.* [21] analyzed the mechanical and tribological characteristics, specifically hardness, wear rate, and friction coefficient, of A356 with Boron Carbide (B4C) and Fly Ash (FA) Metal Matrix Hybrid Composites (MMHC's). The composites were prepared using a stir cum squeeze casting method, with experiments conducted by varying three different equal weight percentages (2.5, 5, 7.5 wt%) of B4C and FA within the A356 alloy. Hardness tests were performed on the prepared samples, while wear and friction characteristics were assessed using a pin-on-disc tribometer, varying the load from 10N to 40N with a constant sliding distance of 2500m. The experimental results showed that hardness increased with an increment in the weight percentage of B4C and FA, with the highest hardness observed in A356 with 7.5 wt% B4C and 7.5 wt% FA MMHC's [22].

The study investigates the effect of incorporating silicon carbide (SiCp) and silicon carbide/alumina ($SiCp/Al_2O_3$) particles on the mechanical and wear properties of composites based on the A356.2 matrix. According to the results, reinforcement boosts the strength, hardness and wear resistance of the material. When seven weight percent SiCp and three weight percent Al_2O_3 were present, the composite had a tensile strength of 134.3 N/mm^2, a hardness of 35 VHN and a wear resistance of 17.27×10^{-5} mm^3/Nm. Optical micrographs demonstrate that the particles are evenly dispersed through the matrix [23].

SIDDHARTHAN *et al.* [24] studied the Metal Matrix Composites (MMCs), which combine the benefits of both metals and ceramics to improve their functionality. Silicon carbide-reinforced aluminium alloy is more rigid and harder and resists wear better than plain aluminium. Because the materials have low residual stresses after processing, this strengthens the bond between the matrix and the reinforcement. The experiments show that specimens with reinforcements are more resistant to wear than those made only of aluminium.

Overall, aluminium ceramic composites are an excellent material with strong and wear-resistant properties that are of great value, especially in the space travel and automotive engineering sectors. This study utilizes the class of materials known as silicon with different-weight parts as reinforcements (0 wt.%, 2 wt.%, 4 wt.%, 6 wt.%, 8 wt.%, and 10 wt.%). Silicon carbide is made possible by using the stir process casting technique. These composites exhibit certain mechanical properties that were investigated, and their construction was examined using tensile strength. Flexural strength, hardness analysis, impact strength, low velocity impact analysis, scanning electron microscopic analysis, and acoustic emission analysis.

2. MATERIALS AND METHODS

2.1. Materials used

A356.2 Aluminium, a commercial grade with a density of 2.7 g/cm^3, is used as a matrix for high-quality metal materials in aerospace, transportation, and marine applications because it is rugged, highly weldable and extremely resistant to corrosion. The contents of A356.2 are provided in Table 1, and the physical, mechanical, and thermal properties of A356.2 aluminium alloy are provided in Table 2. Because it is so hard, SiC is chosen as the reinforcing ceramic material. SiC weighs 3.21 grams per cubic centimetre and melts at 2730°C.

2.2. Fabrication of composites

All specimens used for mechanical characterization are prepared through a stir-casting process. Table 3 presents the code that was used to create the MMCs. Since stir casting is performed in a closed crucible, the crucible chosen for the experiment has a diameter of 120 mm. A composite is manufactured using A356.2 aluminium as the base material and reinforced with 5µm-sized silicon carbide particles. As shown in Figure 1, the stir casting setup, specimen materials, testing samples, and testing equipments are as follows. The experimental setup consists of a three-phase electrical heating furnace, a graphite crucible, a motor, and a mechanical stirrer. Both aluminium and SiC are first cleaned before mechanical stirring. SiC particles underwent to NaOH etching (10% solution for 1 hour) to promote interfacial adhesion and reduce porosity. Once the scraps of aluminium had been cleaned, they were preheated to 450 °C, while SiC were preheated to 1000 °C. Having the component warm up forces the matrix and reinforcement to separate and stay apart. The molten aluminium alloy was mechanically stirred using a graphite-coated impeller at a speed of 600 rpm and maintained for 12 minutes to ensure uniform dispersion of reinforcements while minimizing gas entrapment. The graphite box was used in stir casting and filled with aluminium scraps. Then, the temperature was raised to 750 °C to melt the scraps completely. Melted A356.2 aluminium was mixed with preheated SiC. A small amount of SiC was included in the mixture to make the SiC coatings easier to wet. The SiC ceramic reinforcement particles were preheated at 800 °C for 1 hour in a muffle furnace before addition. Preheated reinforcements were gradually introduced into the vortex formed in the melt to avoid agglomeration and particle settling. After that, the slurry was put into the heated mould to create the form required by ASTM requirements for tensile and impact strength testing. Solidification in the

Table 1: Constituents of A356.2.

Si	Fe	Cu	Mn	Mg	Cr	Ni	Zn	Ti	Al
7.32	0.182	0.111	0.0340	0.358	0.00390	0.0240	0.0190	0.135	Bal

Table 2: Physical, mechanical, and thermal properties of A356.2 aluminium alloy.

SL. NO.	PROPERTY	VALUE
1	Density	2.68 – 2.75 g/cm^3
2	Tensile Strength	220 – 310 MPa (32 – 45 ksi)
3	Yield Strength	140 – 275 MPa (20 – 40 ksi)
4	Elongation	2 – 12% (depending on temperature and heat treatment)
5	Hardness	70 – 100 HB (Brinell Hardness)
6	Modulus of Elasticity	70 – 80 GPa (10.1 – 11.6 × 10^6 psi)
7	Shear Strength	150 – 200 MPa (22 – 29 ksi)
8	Poisson’s Ratio	0.33
9	Ultimate Strength	310 MPa (45 ksi)
10	Thermal Conductivity	150 – 180 W/m·K
11	Specific Heat Capacity	0.897 J/g·K
12	Melting Point	570 – 650°C (1058 – 1202°F)
13	Coefficient of Thermal Expansion	22.5 × 10^{-6} /°C (12.5 × 10^{-6} /°F)
14	Electrical Resistivity	0.039 ohm·mm^2/m (at 20°C)

Table 3: Constituent and coding details of MMCs.

SL. NO.	COMPOSITION OF COMPOSITE	TOTAL WEIGHT OF EACH SAMPLE (G)	A356.2 (%)	SIC (%)	CODING
1	Al base (alloy)	145.8	100	0	Al
2	Al + 2% by wt SiC	145.8	98	2	Al 2SiC
3	Al + 4% by wt SiC	145.8	96	4	Al 4SiC
4	Al + 6% by wt SiC	145.8	94	6	Al 6SiC
5	Al + 8% by wt SiC	145.8	92	8	Al 8SiC
6	Al + 10% by wt SiC	145.8	90	10	Al 10SiC

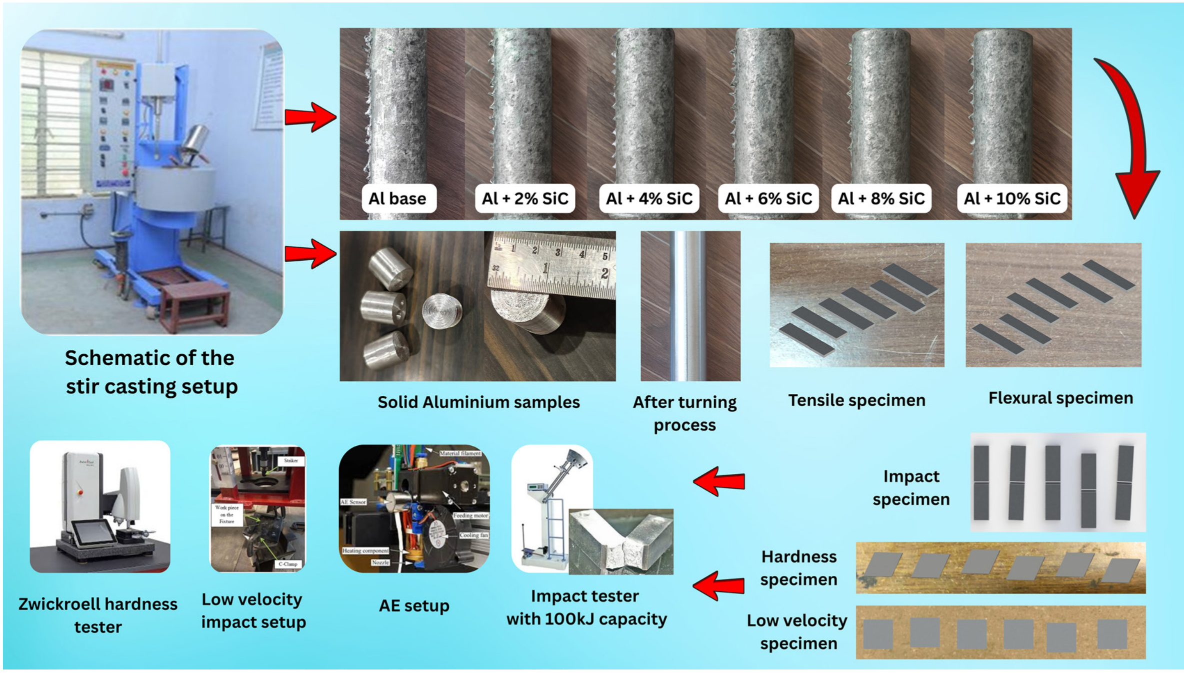

Figure 1: Schematic of the stir casting setup, specimen materials, testing samples, and testing equipments.

moulds took place, and after that, the specimens were cleaned for additional examination. Data is gathered using multiple combinations of process parameters, and samples are prepared for observation under a microscope as well as for mechanical testing.

2.3. Density and porosity of composites

Composites' density was checked using Archimedes' principle, and their theoretical density values were obtained by applying the rule of mixture in accordance with the percentage of reinforcement in each batch (see Equation (1)).

$$\rho_c = \rho_m V_m + \rho_r V_r \quad (1)$$

ρ_c = composite density
ρ_m = density of matrix
V_m = density of reinforcement
ρ_r = mass of composite
V_r = mass of reinforcement

The material's porosity significantly shapes its mechanical and tribological properties. The porosity of composites depends mainly on the method of mechanical alloying, the amount of pressure used, and the sintering temperature. The express form shown in Equation (2) was used to identify the composites' porosity percentages [25].

$$Porosity = \left(\frac{(Theoretical\ density - Experimental\ density)}{Theoretical\ density} \right) \times 100 \quad (2)$$

2.4. Tensile strength of composites

The standard outlines the procedure for tensile testing of metals, as specified in ASTM E08-8 [26]. An Instron Universal Testing Machine was used to conduct the tensile tests with a capacity of approximately 300 kN. Specimens for the tests were 13 mm wide. We measured the specimens at a length of 55 mm. The tests were done according to the guidelines in ASTM E08-8. Both the stress and elongation data were collected using the machine to evaluate the tensile properties of the material. The average results of 5 specimens are used to calculate the tensile studies.

2.5. Flexural strength of composites

Using a flexural test, the behaviour of the materials was checked under three-point bending loading conditions with the customized fixture in the Instron Universal Testing Machine. Ensuring the specimen followed ASTM A370 [27] (200 mm gauge length) guidelines ensured that it had the same structure for each test. Using this standard enables the reliable comparison of different metal matrix composites (MMCs) under bending stress. While testing, the way the material resisted bending before fracturing or changing shape was carefully observed. The average values obtained from five test specimens were considered for evaluating the flexural properties.

2.6. Impact strength of composites

The impact of the Izod sample was tested using the Krystal Impact Tester, according to the ASTM D256 [28] standard. The specimen was 60 mm long, 13 mm wide and 3 mm thick. The test aimed to assess how the metal matrix composite (MMC) withstands impact. The Izod impact test measures the amount of energy a material can absorb when it is rapidly struck. The average values obtained from five test specimens were considered for evaluating the impact properties. A pendulum is built into the apparatus to hit the specimen with absolute height and speed. This data demonstrates the toughness and fracture resistance of different MMCs for various engineering applications.

2.7. Hardness strength of composites

The hardness test is conducted according to ASTM E10-18 [29], using a specimen measuring 10 mm x 5 mm x 1 mm. The Zwickroell hardness tester is a device utilized to conduct hardness indentation tests on composites. Each sample's hardness (Brinell hardness, 500 kgf load) was measured at five different random sites. The specimen surfaces were ground successively with SiC emery paper (grit size 1000), followed by polishing with an alumina suspension to achieve a mirror-like finish. Final specimens were cleaned with ethanol and air-dried to remove residual particles. This surface preparation minimized the effect of surface roughness on indentation response.

2.8. Low velocity impact analysis

To perform low-velocity impact tests, a drop-weight impact machine (RB-310 DWIT from R&B Korea in Korea) was used [30]. To look at how behaviour changes when crack initiation begins, the plate was impacted by 10J until the target crack started to form. All the low-velocity impact tests used a semi-hemispherical indenter with a diameter of 12.7 mm. A square sample of size 100mm × 100mm was made and placed between two square frames. The average values obtained from five test specimens were considered for evaluating the low-velocity studies [31].

2.9. Morphological analysis of composites

To study the surface, the microstructural analysis was carried out using a Σ version–Carl Zeiss Scanning Electron Microscope (Germany, Model EVO MA 15) operated at an accelerating voltage of 15 kV [32, 33]. The magnification range was 500× to 5000×, with a working distance of 8–10 mm. A Secondary electron (SE) imaging mode was employed to reveal surface morphology under high-vacuum conditions using a Beta-Field Emission Scanning Electron Microscope (FESEM) in this research. The Bruker-04 TASMAN Energy Dispersive X-ray Spectroscopy (EDS or EDAX) instrument was used for spectral analysis to map the elements in the stem fiber. Assembling the equipment follows the arrangement of the FESEM setup.

2.10. Acoustic emission analysis of composites

The Vallen AMSY4 system and the Instron 1195 were directly coupled via parametric input, allowing for real-time monitoring of AE activity versus load data. A full-scale load cell range set to 50kN and the crosshead displacement rate was 0.5mm/min. All tests used a sampling rate of 0.625 MHz/s and a 35.5dB threshold. The data was analyzed using the Visual AE application within the VALLEN software, which allowed multiple AE parameters to be plotted against one another for analysis [34]. Figure 2 shows the AE setup.

3. RESULTS AND DISCUSSION

3.1. Density and porosity analysis of composites

The difference in the theoretical density and experimental density of Al7075/SiC composites is shown in Figure 3a. The addition of SiC filler to the aluminum matrix likely increases the overall density of the composite compared to pure aluminum, as SiC has a higher density (~3.21 g/cm^3) than aluminum (~2.70 g/cm^3). The graph

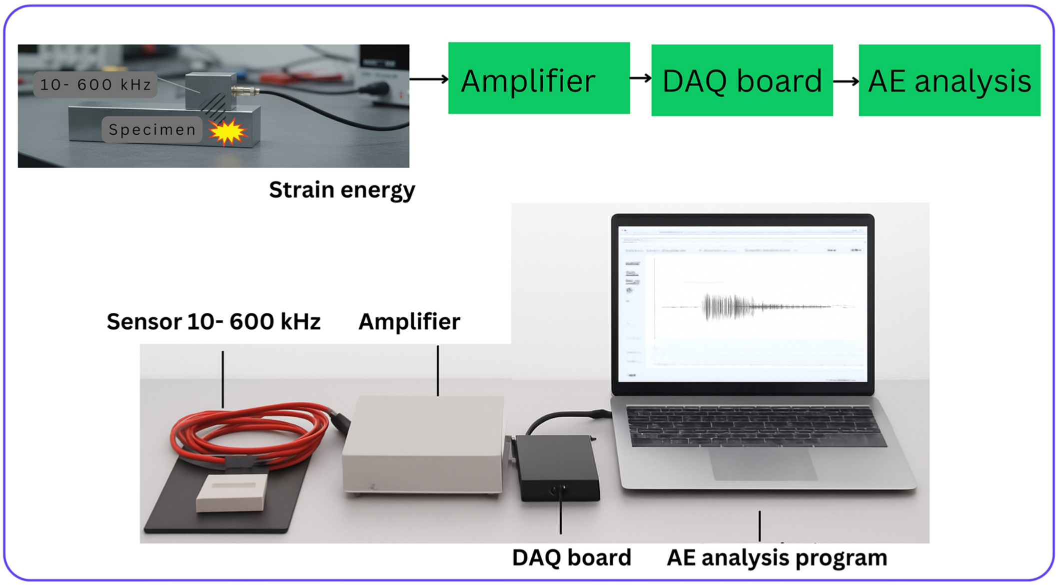

Figure 2: Acoustic emmision setup.

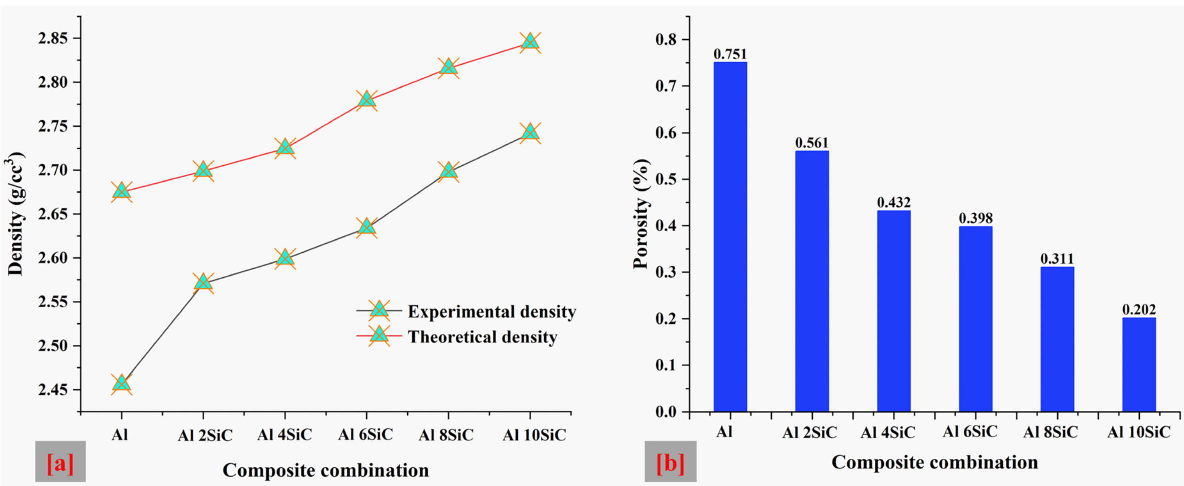

Figure 3: (a) Density & (b) porosity comparison of composite combinations.

suggests a gradual increase in density with increasing SiC content, indicating a direct correlation between filler concentration and composite density. The minimum and maximum experimental density are 2.456 and 2.742 g/cm^3, where the minimum and maximum theoretical density are 2.675 and 2.845 g/cm^3, respectively. This trend corroborates earlier studies, which found that ceramic reinforcements, such as SiC and Al_2O_3 enhance composite density [35]. However, the current work may provide new insights into the threshold at which density gains outweigh lightweight advantages.

Porosity tends to decrease with higher SiC content due to better particle packing and reduced voids in the composite structure shown in Figure 3b. The porosity for the used combination in this research dropped gradually from 0.751 to 0.202 %. However, excessive SiC loading may lead to agglomeration, resulting in localised porosity increases, which could be visible in the graph when comparing multiple compositions. A denser composite with lower porosity generally exhibits improved mechanical properties (e.g., hardness, strength) due to enhanced interfacial bonding between Al and SiC. The Al-SiC composite exhibits a predictable increase in density with SiC reinforcement, accompanied by a reduction inorosity at optimal filler levels [36-38]. This suggests improved material performance for applications that require lightweight yet strong components, such as those in aerospace or automotive parts. Further studies could explore the effects of particle size and distribution on porosity for refinement.

3.2. Tensile strength analysis

The presence of silicon carbide (SiC) filler causes the Al matrix composites to become stronger, and this increase is noticeable as the amount of SiC increases (refer to Table 4 and Figure 4). The tensile strength of Pure Al is 280.64 MPa, but SiC increases that strength greatly. Al-10SiC (10 % SiC) has the best tensile strength (349.57 MPa), showing an increase of ~24.5 % compared to pure Al. This indicates that the strength is directly related to the SiC content due to load transfer, dispersion strengthening and a few interfacial flaws. Maximum deflection is reduced more and more as the amount of SiC is increased in the composites [39]. The Pure Al material can be bent to a larger extent (8.35 mm), making it the most ductile, whereas Al-10SiC is the least ductile (only to a deflection of 3.77 mm). A decrease in ductility happens because SiC particles in the metal limit the deformation process. The presence and movement of particles within the crystal cause high stress around them, leading to

Table 4: Tensile properties of composites.

SL. NO.	SAMPLE	TENSILE BREAKING LOAD (KN)	MAXIMUM DEFLECTION (MM)	TENSILE STRENGTH (MPA)	ERROR (%)
1	Al	55.26±5.02	8.35±0.9	280.64±2.8	4.69
2	Al 2SiC	56.97±5.96	8.21±0.82	310.85±3.1	2.89
3	Al 4SiC	59.28±4.96	7.89±0.69	314.29±2.9	6.41
4	Al 6SiC	61.79±5.6	6.88±0.596	326.46±3.6	5.39
5	Al 8SiC	62.88±6.1	5.12±0.45	341.56±3.7	7.8
6	Al 10SiC	64.29±6.45	3.77±0.26	349.57±3.69	6.66

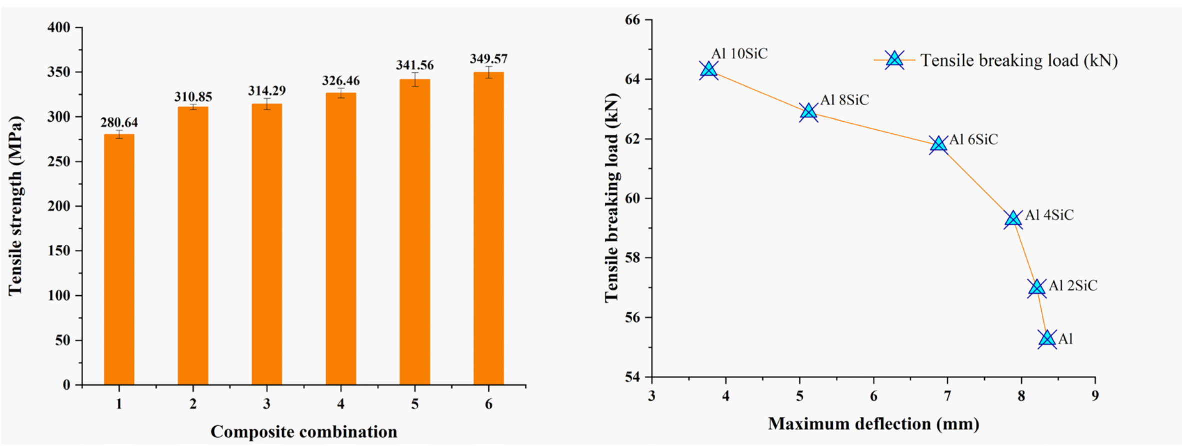

Figure 4: Tensile strength comparison of composite combinations.

a faster fracture [40]. BARADESWARAN *et al.* [41] discussed that research on stir-cast Al (e.g., 6061, 7075 alloys) reinforced with SiC particles consistently reports an increase in tensile strength with increasing SiC content up to a certain limit, often around 10-15 wt%. Industrial Implications recommends using Al-4SiC for moderate flexing and Al-8SiC for high-load situations. The way an application is built is determined by what it needs to do. An example is Al-6SiC, which exhibits balanced features (326.46 MPa strength and 6.88 mm deflection). Other research could investigate the use of nanoscale SiC or hybrid additions to mitigate a decrease in ductility without compromising the added strength.

3.3. Flexural strength analysis

There is a clear pattern in Table 5 and Figure 5, indicating that the flexural strength rises as the SiC filler is added to the aluminium matrix (Al). Al-10SiC shows a 108.8% higher flexural strength than pure Al thanks to the good reinforcement effect of SiC. Greater flexural strength is seen in aluminium with SiC (up to 240.85 MPa for Al-10SiC), confirming that SiC is an effective reinforcement. This is consistent with classical composite theories, which suggest that hard particles impede the movement of dislocations, thereby strengthening the materials [42]. It is found that SiC particles hinder the movement of dislocations in the Al matrix, thereby improving load-bearing capacity. As more SiC is added (Al-8SiC to Al-10SiC), the improvement in strength slows down, possibly due to the grouping of particles or problems at the particle interfaces. Plastic deformation is prevented by SiC in the Al matrix, which means the metal becomes stronger but less tough [43]. The addition of more SiC in the materials causes them to bend less, making the composites more rigid. It can be noted that as strength increases, the ability to deform decreases by nearly half (from 11.05 mm to 4.98 mm), making this material unsuitable for applications where deformation is essential [44]. Hence, Al-6SiC to Al-8SiC has the best proportions because it gives the right mix of strength (201–218 MPa) and moderate deflection (6.41–8.89 mm). This research may inform the formulation of SiC-reinforced Al powder suitable for 3D printing, considering both its printing quality and mechanical performance.

Table 5: Flexural properties of composites.

SL. NO.	SAMPLE	FLEXURAL BREAK LOAD (KN)	MAXIMUM DEFLECTION (MM)	FLEXURAL STRENGTH (MPA)	ERROR (%)
1	Al	1.78 ± 0.2	11.05±1.2	115.48±8.3	3.25
2	Al 2SiC	2.01±0.4	10.89±0.89	137.58±9.6	2.18
3	Al 4SiC	2.89±0.96	10.06±0.95	180.69±17.5	3.85
4	Al 6SiC	3.41±0.35	8.89±0.8	201.47±18.5	1.08
5	Al 8SiC	3.84±0.25	6.41±0.54	218.45±20.6	1.56
6	Al 10SiC	4.02±0.04	4.98±0.58	240.85±23.7	-

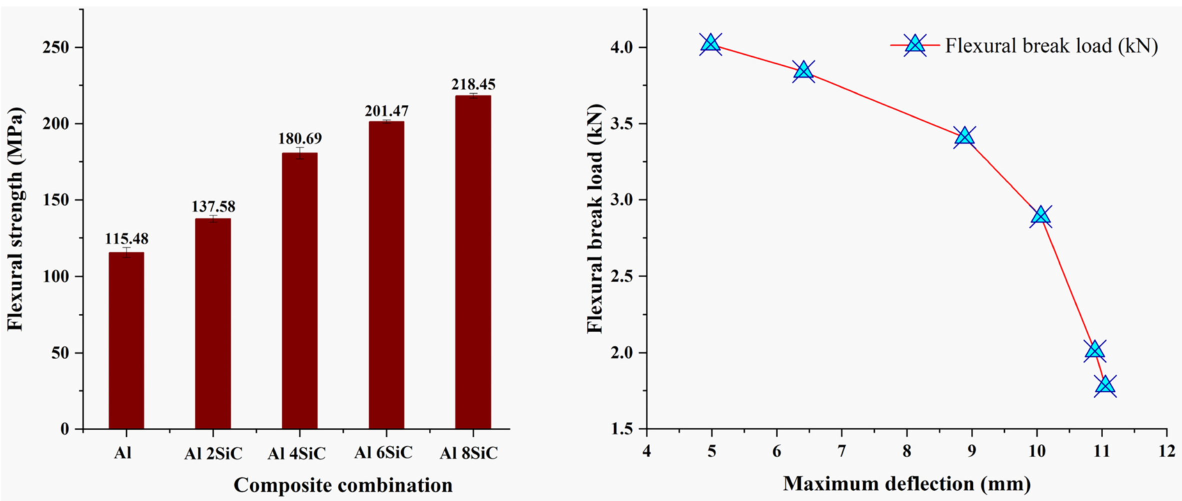

Figure 5: Flexural strength comparison of composite combinations.

3.4. Impact strength analysis

Figure 6 displays the strength of aluminium (Al)-based composites that have been strengthened with silicon carbide (SiC) filler. Table 6 provides the details of the toughness properties of composites. The research tested mixtures made of six composite combinations, each with a different SiC proportion (0% to 10%). Aluminium (0% SiC) had an impact strength of 47.53 kJ/m^2. Still, as the SiC content increased (2% SiC: 48.91 kJ/m^2, 4% SiC: 50.63 kJ/m^2, 6% SiC: 51.78 kJ/m^2, 8% SiC: 52.79 kJ/m^2 and 10% SiC: 53.68 kJ/m^2), the impact strength. The higher proportion of SiC in the powder allows the aluminium to become tougher, which suggests that SiC particles serve as proper reinforcements [45]. Crack growth is probably slowed down by SiC, allowing stress to be spread more uniformly inside the material during impact [46]. Its growing impact strength means that a composite with 10% SiC reduces the risk of brittleness seen in composites with too much fiber content. The impact strength of aluminium composites is much greater when given SiC reinforcement, and this effect is best seen when the filler amount reaches 10% [47]. KOK *et al.* [48] and other researchers typically report a significant decrease in Charpy impact strength as the SiC content rises. For instance, the impact energy of an Al alloy might drop by 30-50% with the addition of 10 wt.% SiC. This is attributed to the embrittling effect of the ceramic particles. Studies may be conducted to determine the maximum SiC concentration at which brittleness becomes too significant an issue.

3.5. Hardness strength analysis

Table 7 and Figure 7 show the hardness of Al composites filled with silicon carbide (SiC) filler at various ratios. The hardness increases with an increase in silicon carbide content. The hardness of pure aluminium is 83.15–84.12 BHN, and it rises as the amount of silicon carbide (SiC) is increased. Using more SiC significantly

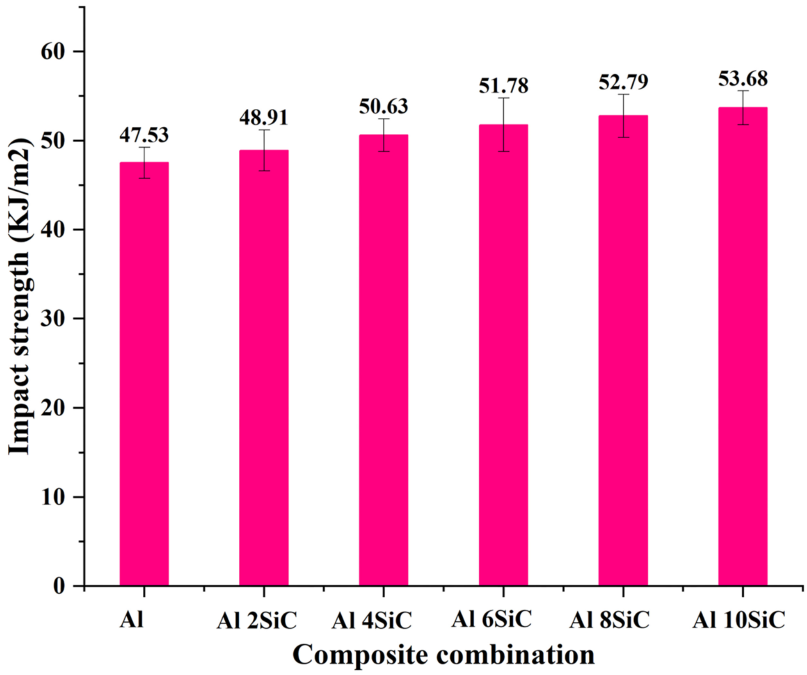

Figure 6: Impact strength of composite combinations.

Table 6: Toughness properties of composites.

SL. NO.	SAMPLE	IMPACT STRENGTH (KJ/M2)	ERROR (%)
1	Al	47.53±3.65	1.75
2	Al 2SiC	48.91±4.20	2.29
3	Al 4SiC	50.63±3.69	1.84
4	Al 6SiC	51.78±4.8	3.01
5	Al 8SiC	52.79±4.6	2.41
6	Al 10SiC	53.68±4.4	1.89

Table 7: Hardness properties of composites.

SL. NO.	SAMPLE	BRINELL HARDNESS NUMBER (BHN)	ERROR (%)
1	Al	83.15±7.6	1.36
2	Al 2SiC	84.12±7.9	2.01
3	Al 4SiC	86.98±7.85	1.98
4	Al 6SiC	90.12±8.3	1.08
5	Al 8SiC	94.82±8.95	2.69
6	Al 10SiC	101.25±9.36	2.84

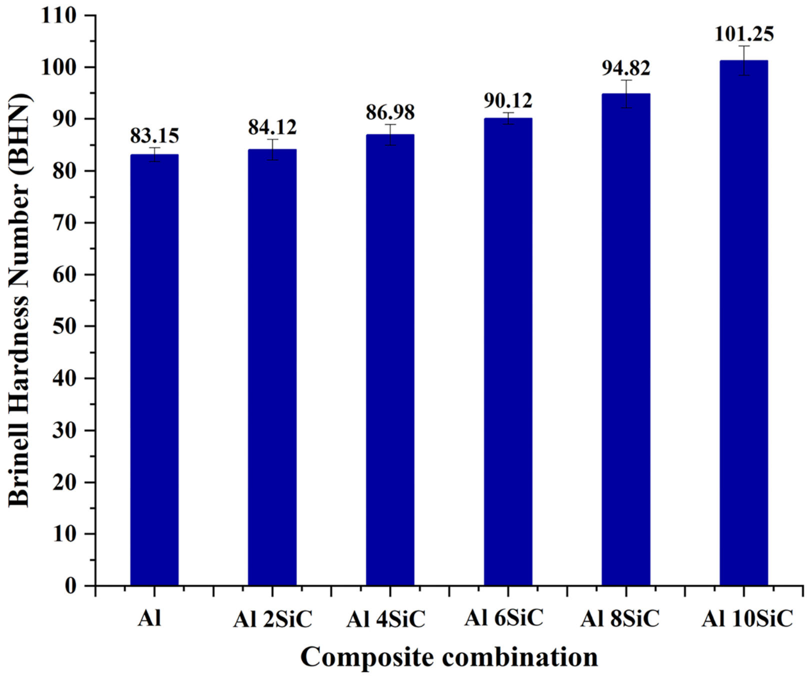

Figure 7: Hardness properties of composite combinations.

raises the Vickers hardness: Al-2SiC (84.12 BHN), Al-4SiC (86.98 BHN), Al-6SiC (90.12 BHN), Al-8SiC (94.82 BHN), and Al-10SiC (101.25 BHN). With 10% Silicon Carbide, the hardness reaches its highest level (101.25 BHN) and is about 22% better than pure Al. Because SiC particles block the movement of dislocations, more hardness is produced in the Al-SiC metal. Because SiC is a hard ceramic, it enhances the composite's ability to resist deformation [49]. The clear connection between SiC content and hardness shows that the matrix has a strong transfer of load to the reinforcement. The greater the SiC content, the more sites there are for stress to be distributed, which makes the material harder [50, 51]. The findings demonstrate that using SiC reinforcement in aluminium can help it withstand wear and support heavy loads (e.g., in parts used in cars or planes). The information from testing can help engineers set up Al-SiC for different hardness levels (e.g., 90 BHN for medium-duty and 100+ BHN for heavy-duty uses). The research demonstrates that low SiC content (2–10 weight per cent) results in much higher hardness, which is essential for lightweight structures.

3.6. Low velocity impact analysis

Tests were performed using a low-velocity impact method on samples made from an aluminium (Al) matrix fortified with various amounts of silicon carbide (SiC) filler (0% to 10%), shown in Figure 8. All samples were exposed to an energy of 10 J. The figures display the maximum force (in Newtons, N) recorded during the impact for every type of composite. The force needed to reach the peak increased consistently as more SiC filler was used. Pure Al required less force than any other sample (3233 N), while adding 10% silicon carbide to it revealed the most significant peak force (3533 N). As a result, SiC reinforcement makes the material stronger against being deformed during an impact. The strength and stiffness of the composite were boosted gradually when the SiC content was increased [52]. A nine per cent compression of Al with SiC particles resulted in the

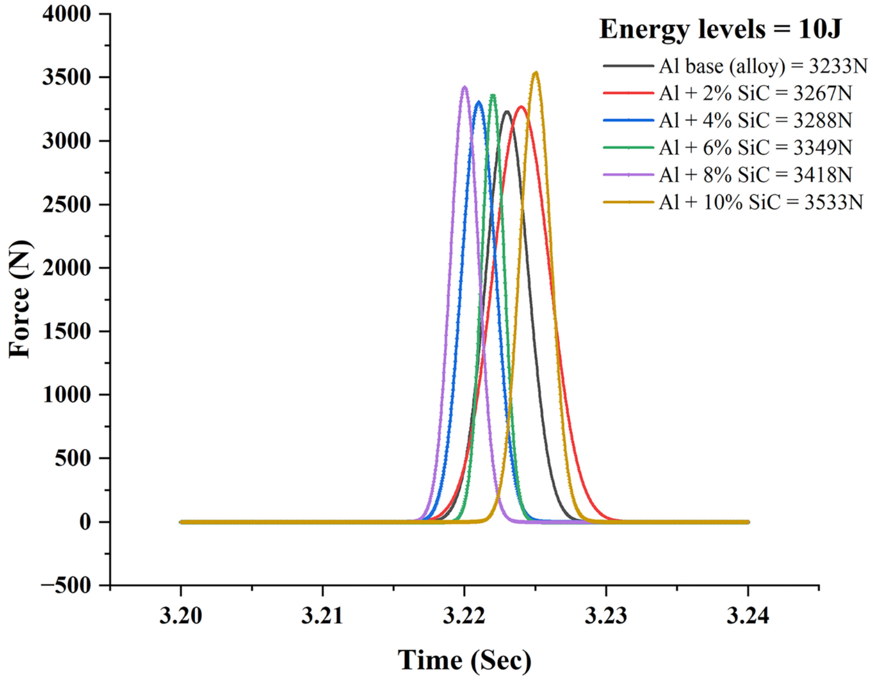

Figure 8: Low velocity impact analysis of composite combinations.

highest improvement, yielding a peak force that was ~9.3% higher than that of pure Al. Because the impact energy (10 J) remained unchanged, the rise in peak force indicates that the composite combines elastic and plastic deformation to utilise energy more efficiently than before. The presence of SiC particles probably slows down crack formation, which increases the toughness of the material [53]. Confirmed through low-velocity impact studies, SiC reinforcement enhances the impact resistance of Al-based composites. The right amount of SiC changes depending on how much strength, mass and flexibility is required for the task.

3.7. Morphological analysis

In Figure 9, SEM fractographs show the fracture surfaces of aluminium matrix composites filled with SiC at different percentages (from 2% to 10%) after undergoing tensile fracture toughness testing. The image of the fracture surface indicates that ductile processes were responsible for breaking, as it displays (2% SiC, 100 nm scale, Fig. 8(a)). Since there is less SiC, the aluminium matrix can be formed or deformed more before it fails. In Fig. 8(e), at 10% SiC, we observe nano-sized cracks (2 nm) and a significant number of particles being pulled out, indicating that the embrittlement is very severe. As there is not enough good adhesion between the composite and the filler, the cohesive strength decreases when there is too much filler [54-56]. When SiC content goes from 2% to 10%, the fracture process shifts from ductile (dominated by the matrix) to brittle (dominated by the filler). Higher SiC content lowers the plasticity of aluminium, which reduces the amount of energy that can be absorbed. Enough SiC particles cause dispersion issues so that the packing of SiC leads to the formation of weak spots where cracks begin to emerge toward the C/D stage. It matters that dispersion is good to prevent things from failing too quickly [57, 58]. A 10% volume of SiC creates a poor fit, so Al and SiC do not adhere well, leading to debonding, making the material more brittle. The research indicates that there is a certain amount (6% and 8% of SiC) above which the mechanical features deteriorate with some pulled-out particles, and crack initiation zones were noticed. At high SiC contents (≥6%), tiny particle groupings produce zones, resulting in the formation of tiny, nano-sized cracks by 10% SiC. It is found that the way Al-SiC particles are incorporated and their interface play a bigger role in fracture behaviour than the content of filler materials. This demonstrates the importance of utilizing innovative processes and modifying the interface to ensure SiC composites are both tough and strong.

3.8. Acoustic emission analysis

The study utilizes composite materials that are powder metallurgy-processed A356.2 aluminium alloys with 2%, 4%, 6%, 8%, and 10% SiC particles. Testing was conducted at room temperature, with the sample's longitudinal axis oriented parallel to the crack growth direction (in the direction of extrusion). Specimens had dimensions of 100 mm × 10 mm × 6 mm, and testing was conducted using an Autograph Universal machine (Shimadzu, Japan)

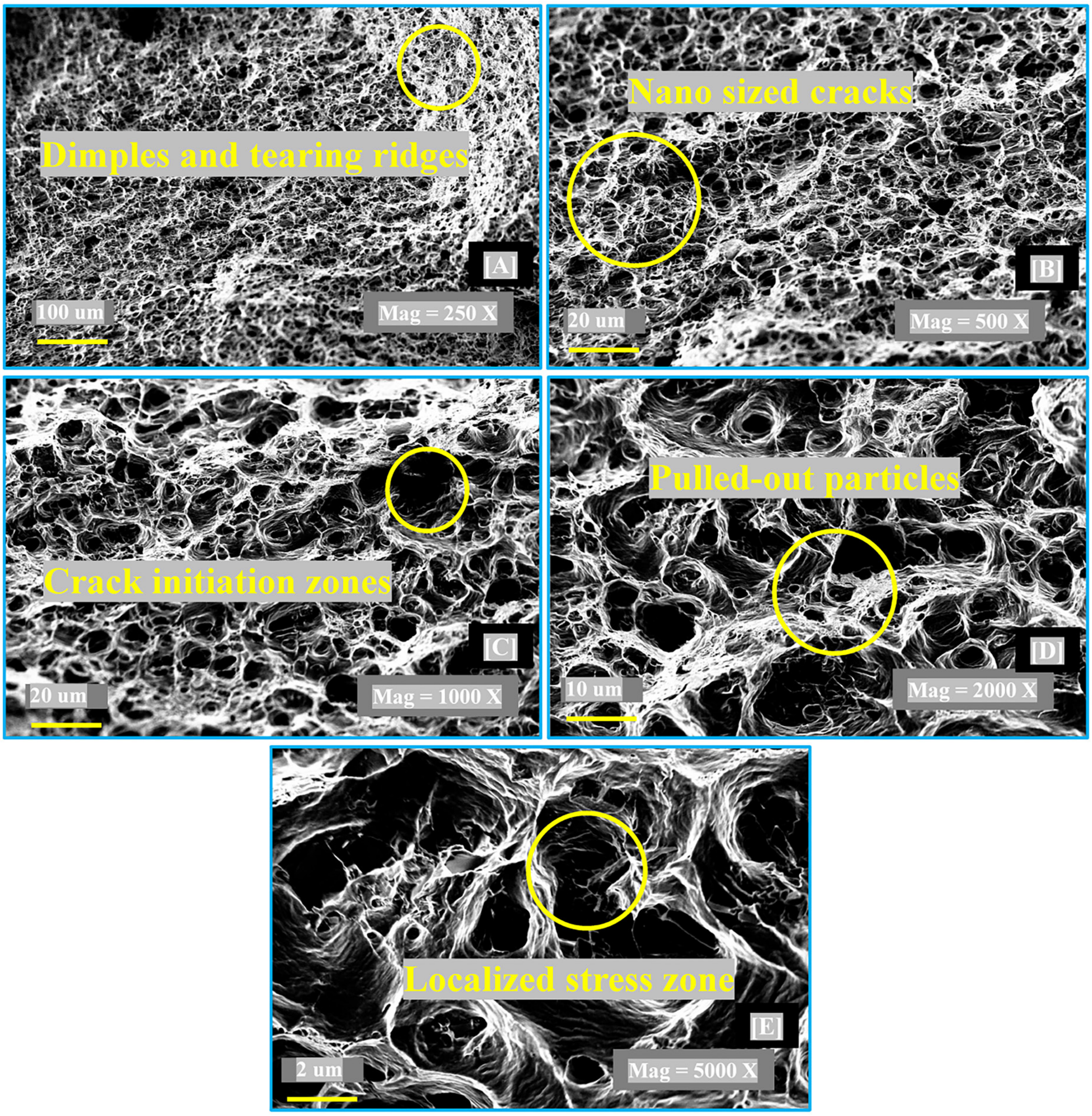

Figure 9: SEM fractographs showing the fracture surface after tensile fracture toughness test on materials reinforced with: (A) 2% of SiC, (B) 4% of SiC, (C) 6% of SiC, (D) 8% of SiC, and (C) 10% of SiC particles.

with a 5 mm crack length and a 60 mm span. During loading, a clip gauge was placed between the knife edges of the sample to monitor crack opening displacement (COD), with a crosshead speed of 0.1 mm/min [59, 60].

While the tensile test is happening, the Two-channel AE source characterization test will be done. The steps in this method are illustrated in Figure 10. After recording the samples with load, the assorted sensors converted these acoustic signals into electrical signals, which were then amplified through preamplifiers to a usable level. This level was subsequently measured using a two-channel computer system. For this study, AE sensors with a Fiji Ceramic head amplifier (gain 54 dB, model M204A, Japan) were used, which also have a resonance frequency of 180 kHz and are 3 mm in size. All sensor output signals were made usable by first being amplified with the low-noise type preamplifier A1002 (Fuji Ceramic) [61]. The signal from the preamplifier was next digitized and sent to the wave memory for storage. Wave memory data was sent from the central memory to the local CPU. A breaking pencil lead was used to calibrate the AE sensors and the measuring system.

Microcracks in materials, as observed in dislocation theory and seismology, can be identified by the seismic moment tensor. It functions similarly to the source function in AE technology. When acoustic signals are sent from a deforming source, they are always changed or distorted when they are picked up by a receiver at some distance. Viscous damping in the material, the reflection effects from the sample's boundaries and

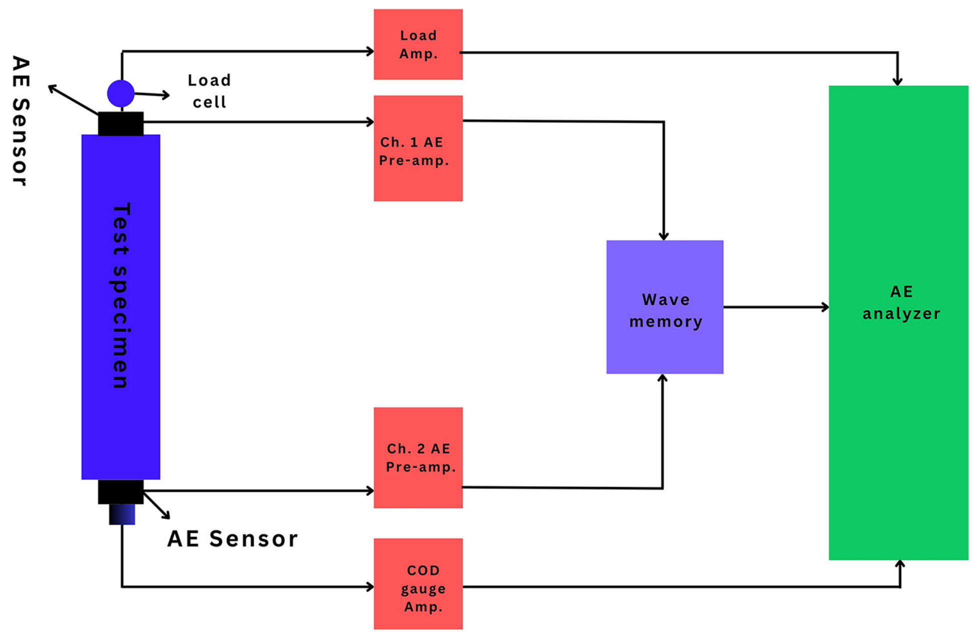

Figure 10: Block diagram of the tensile test method for characterizing the acoustic emission source.

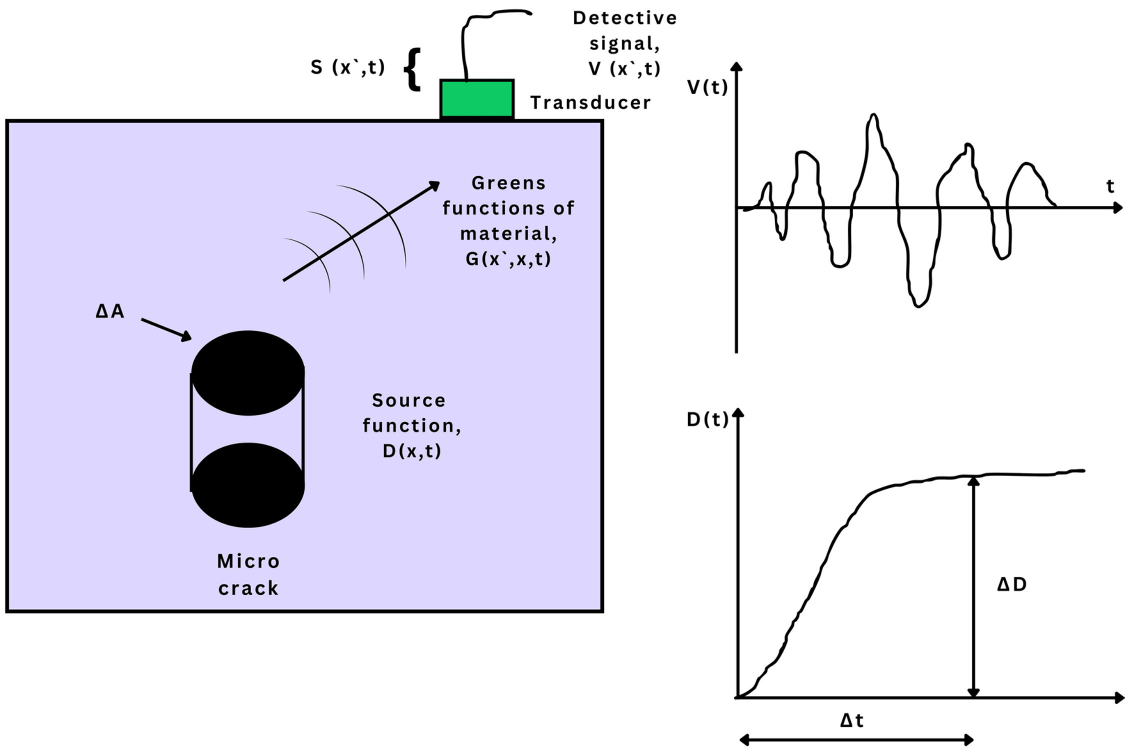

Figure 11: The relationship between the detected signal (V) and the source function (D) in the acoustic emission signal process, where S is the measuring system's response function and G is a dynamic Green's function.

surfaces, as well as the response of the detection system (Figure 11), are common factors that can cause distortion in the measurement. As a result of Equation (3), the voltage observed at a receiver located at x, V (x, t), is said to be a combination of the system's response function, S (x, t), the testing material's Green's function, G (x, x, t) and the moment tensor, D (x, t), as follows:

$$V(x', t) = S(x', t) \times \mathrm{G}(x', x, t) \times D(x,t) \tag{3}$$

The reports indicate that you must deconvolve the AE data from several channels approximately six times to determine the deformation moment tensor. If micro-cracking develops under load in a tensile manner, it is possible to analyze it as a standard linear convolution issue [62]. So, measuring just one channel can tell you how big the cracks are and how quickly they are created. In addition to using moment tensors, a two-channel AE approach was employed to enhance the identification of source locations. Based on how much longer the wave takes to reach one of the transducers, compared to the other, the source of the noise can be found. When scientists locate exact source events, it helps separate unneeded AE ringing and noise from the ringing caused by cracks growing [63, 64].

By using acoustic emission (AE), the research team can see the microstructural changes and fracture pattern in Al-SiC composites as they are subjected to tensile stress. Relating the detected signal (V) with the source function (D) (Figure 9) shows how AE signals relate to internal damage (Figure 10). By looking at the dynamic Green's function (G) and the system's response (S), we can tell that the AE signals are sensitive to both the formation and growth of cracks. More hollow points are observed on fractured surfaces when SiC content is high (e.g., 10%) due to the large number of brittle fractures happening inside the material, including particle separations and the creation of nano-cracks [65]. In this SiC content range (2–4%), AE signals appear less frequently but are more intense, representing areas where fractures are ductile (such as dimples). With a SiC content of 6–10%, AE occurs constantly and features a smaller amplitude, suggesting that SiC particles cause continuous breakage and combine with microcracks [66].

Although it is not discussed in the document, it is possible that the Felicity Effect was seen when the device was reloaded. The existence of SiC particles in a material causes stress accumulation that causes damage that cannot be fixed (for example, debonding at the material's interfaces). Reloading after initial loading can cause AE at lower stresses, indicating that the material has become progressively weaker [67]. When Al-SiC adhesion is poor (observable in 10% SiC), the Felicity Effect happens more easily, since broken interfaces fail faster. The Felicity Ratio (stress after reload/stress before reload) can determine the reliability remaining in Al-SiC parts. An LSR below 1 indicates severe damage, which guides the need for either maintenance or replacement.

AE observation reveals that the fracture behaviour in composites transitions from ductile to brittle, depending on the amount of SiC present. More research on the Felicity Effect could provide valuable insights into the residual strength remaining after testing and the amount of damage incurred during the process. Further studies could investigate mixtures of fillers or even nano-SiC to enhance the bonding between the fibres and reduce the amount of AE that occurs when the material is reloaded.

The Figure 12 depicts the acoustic emission (AE) activity, plotted against time vs hits, provides a detailed account of the damage evolution within the A356.2 alloy and its SiC-reinforced composites. The AE data, segmented into three regions, allows for a high-resolution analysis of the underlying failure mechanisms. The AE signature for the unreinforced Al alloy (Al) is expected to be dominated by events related to matrix plastic deformation and the fracture of brittle silicon particles in the eutectic phase [68]. The onset of significant AE activity would likely correspond to the yield point, with a sustained release of energy during plastic deformation until final fracture. In general, the cumulative AE energy and event count are expected to increase with higher SiC content, especially in the early and middle stages of deformation. This can be attributed to several key factors like particle fracture, matrix/interface debonding, and plastic deformation of the matrix. The initial regions (0-100s) likely correspond to the elastic loading phase and the very early stages of plastic deformation. AE activity here is typically low but may contain initial particle fractures or interface debonding events in the higher SiC content composites, indicating early damage initiation [69]. In region 100-300s, composites with higher SiC content (Al 6SiC to Al 10SiC) are expected to show sustained high-energy AE activity due to continuous particle fracture and interface failure. In contrast, the Al 2SiC and Al 4SiC composites might show a more moderated but increasing level of activity. The third region correspond to the final fracture and necking phase. A massive, high-energy burst of AE signals is expected across all samples, coinciding with the unstable crack propagation and ultimate failure of the specimen. The composite Al 4SiC appears to show a different AE profile in the legend, which may indicate a more optimal reinforcement level where the benefits of load transfer from the matrix to the particles are maximized before excessive particle fracture becomes the dominant failure mode.

The AE parameter θ represents the cumulative signal energy generated during deformation and fracture, directly corresponding to the microstructural activity such as matrix yielding, particle–matrix interface debonding, and crack propagation. Across all compositions, the AE response follows a three-stage pattern; initial rise region (0–100 s), plateau region (100–300 s), and drop region (>300 s) [70]. The pure Al sample (Figure 13(a)) exhibits the highest AE peak intensity (~3000 mV), reflecting a pronounced ductile behavior with significant dislocation-based activity before failure. With the progressive addition of SiC reinforcement (2–10 wt %), a noticeable shift in AE pattern is observed. The composites show a slightly reduced peak AE amplitude and a shorter duration of the plateau region, suggesting an increase in stiffness and a reduction in plastic deformation

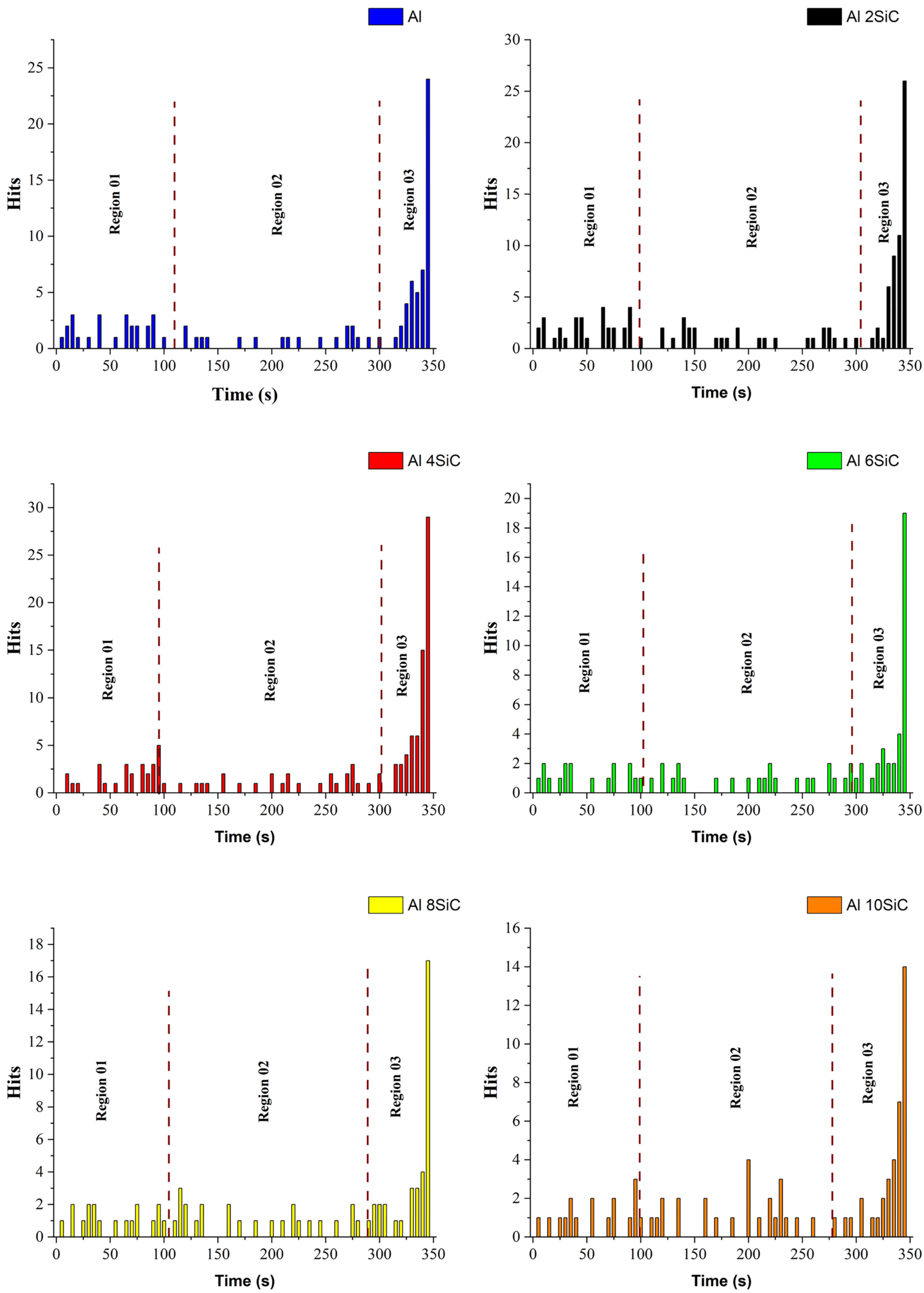

Figure 12: Regional level time (s) *vs* hits of acoustic emission (AE) activity.

capacity [71, 72]. The Al 2SiC and Al 4SiC samples maintain relatively high AE responses, indicating effective stress transfer between the matrix and reinforcement. However, for Al 6SiC–Al 10SiC, the AE amplitude slightly decreases, which can be attributed to particle clustering and reduced interfacial bonding efficiency at higher SiC

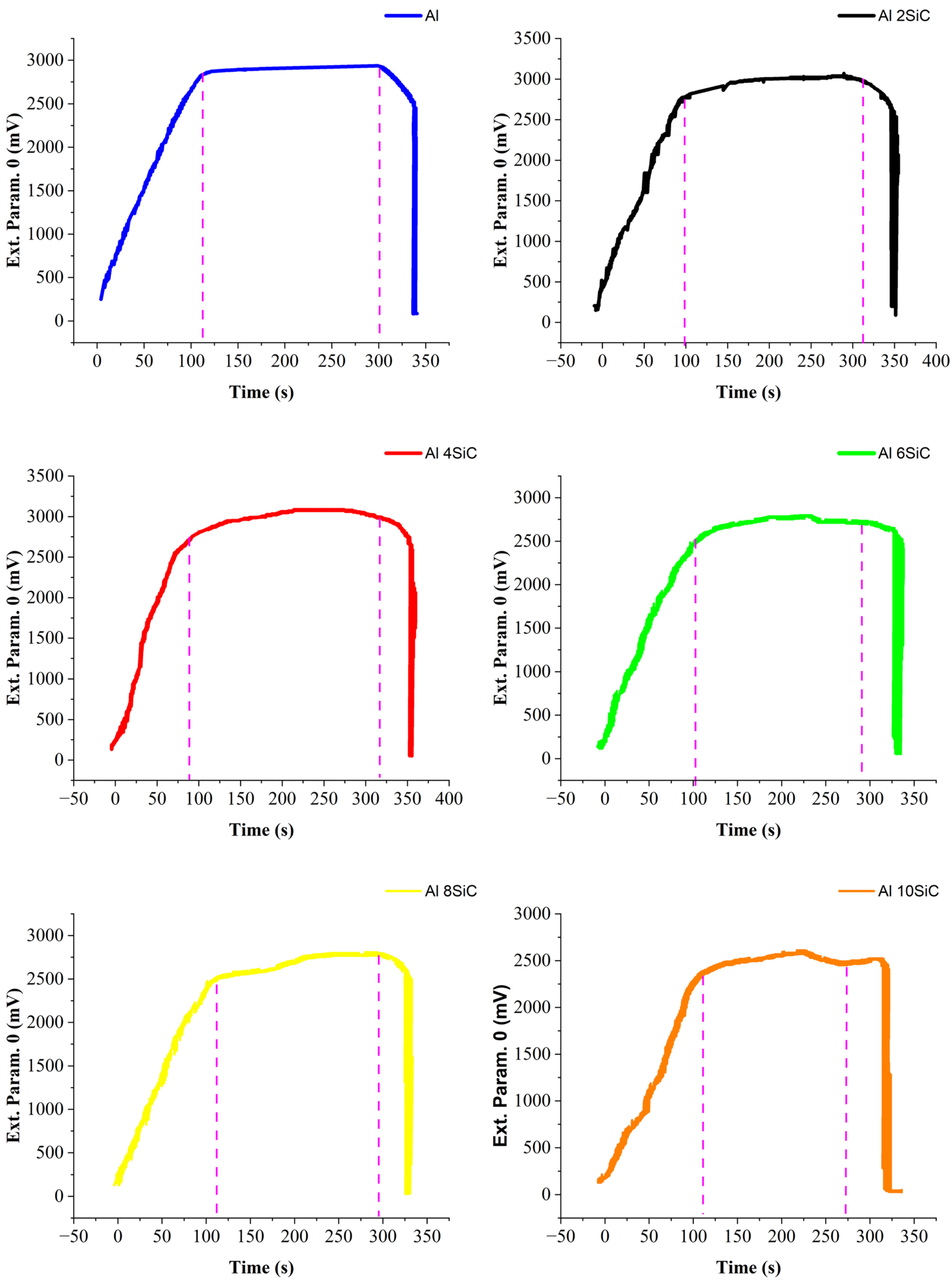

Figure 13: The variation of the AE extracted parameter (θ, mV) with respect to time.

contents [73]. Despite this, these composites demonstrate higher resistance to crack initiation, confirmed by the delayed AE onset and consistent plateau behavior. Overall, the AE analysis confirms that increasing SiC content enhances the composite's stiffness and load-bearing capacity while slightly compromising ductility. The AE signal characteristics effectively capture the transition from ductile matrix deformation (Al) to more brittle fracture behavior (Al 10SiC). The steady AE response between 100–300 s across all samples indicates stable composite integrity before catastrophic failure, demonstrating the reliability of AE monitoring for damage progression studies in metal matrix composites.

4. CONCLUSIONS

This study shows that alumina-based MMCs processed by stir casting exhibit significant mechanical improvements with SiC reinforcement up to 10%. Increased SiC enhances strength, toughness, and impact resistance, while reducing ductility and shifting fracture from ductile to brittle due to SiC–matrix interfacial effects. Intermediate levels (6–8%) provide the best balance of strength and flexibility. Acoustic emission results further confirm SiC's role in crack propagation and damage accumulation. The A356.2 alloy with 4-6% SiC reinforcement demonstrates an optimal balance, enhancing strength without excessive brittleness.Although the composites show strong potential for lightweight, high-performance components, aerospace and automotive suitability requires component-level validation and benchmarking with industrial requirements. Future work should explore hybrid or nanoscale reinforcements to reduce brittleness, expand the reinforcement range, alternative SiC.

5. ACKNOWLEDGEMENT

This research was supported by the Department of Mechanical Engineering, Rohini College of Engineering and Technology, Palkulam, Anjugramam-629401, kanniyakumari, Tamil Nadu, India.

This research received no specific grant from any funding agency in the public, commercial, or not-for-profit sectors.

6. BIBLIOGRAPHY

[1] NARTU, M.S.K.K.Y., AGRAWAL, P., "Additive manufacturing of metal matrix composites", *Materials & Design*, v. 252, pp. 113609, 2025. doi: https://doi.org/10.1016/j.matdes.2025.113609.

[2] ANNAPOORNA, K., ANANDA, R., DESHPANDE, V., *et al.*, "Nano reinforced aluminium based Metal Matrix Hybrid Composites: an overview", *Journal of Physics: Conference Series*, v. 2748, n. 1, pp. 12007, 2024. doi: https://doi.org/10.1088/1742-6596/2748/1/012007.

[3] SANKAR, T., MOHANAVEL, V., "Enhanced mechanical and wear characteristics of AZ61/Si3N4 composites through stir casting technique and RSM modeling", *Matéria*, v. 30, pp. e20240736, 2025. doi: https://doi.org/10.1590/1517-7076-rmat-2024-0736.

[4] WU, X., ZHANG, W., "A review on aluminum matrix composites' characteristics and applications for automotive sector", *Heliyon*, v. 10, n. 20, pp. e38576, 2024. doi: https://doi.org/10.1016/j.heliyon.2024.e38576. PubMed PMID: 39640838.

[5] KAREEM, S.A., ANAELE, J.U., AIKULOLA, E.O., *et al.*, "Aluminium matrix composites reinforced with high entropy alloys: a comprehensive review on interfacial reactions, mechanical, corrosion, and tribological characteristics", *Journal of Materials Research and Technology*, v. 30, pp. 8161-8186, 2024. doi: https://doi.org/10.1016/j.jmrt.2024.05.153.

[6] ADIL, M.M., HASSAN PARVEZ, M.M., HASSAN, M.M., *et al.*, "Effect of jute stick charcoal powder on characterization of aluminum metal matrix composite", *Results in Engineering*, v. 22, pp. 101990, 2024. doi: https://doi.org/10.1016/j.rineng.2024.101990.

[7] ARUNPRASATH, K., AMUTHAKKANNAN, P., SUNDARAKANNAN, R., *et al.*, "Mechanical, wear, and low-velocity impact studies of AL7075/Basalt/Mica particle hybrid metal matrix composite through stir casting route", *Journal of Materials Engineering and Performance*, v. 34, pp. 11420–11432, 2025. doi: https://doi.org/10.1007/s11665-024-09951-0.

[8] ANBUMANI, P., BABBAR, A., ARUNPRASATH, K., *et al.*, "Finite element modeling and analysis of crashworthiness performance of bioinspired thin-walled tapered tubular structures.", *International Journal on Interactive Design and Manufacturing*, 2024. doi: https://doi.org/10.1007/s12008-023-01727-5.

[9] SANKHLA, A.M., PATEL, K.M., MAKHESANA, M.A., *et al.*, "Effect of mixing method and particle size on hardness and compressive strength of aluminium based metal matrix composite prepared through powder metallurgy route", *Journal of Materials Research and Technology*, v. 18, pp. 282–292, 2022. doi: https://doi.org/10.1016/j.jmrt.2022.02.094.

[10] VELLAICHAMY, R., SUDARSAN, D., THEERKKA THARISANAN, R., *et al.*, "Investigate the mechanical properties of Aluminium Metal Matrix Composite", *Journal of Physics: Conference Series*, v. 2748, n. 1, pp. 12009, 2024. doi: https://doi.org/10.1088/1742-6596/2748/1/012009.

[11] FERNÁNDEZ-GARCÍA, C., PADILLA-ENCINAS, P., FERNÁNDEZ, R., *et al.*, "Interaction of aluminum alloys with MKPC and Portland-based cements on the metal-matrix interface", *Applied Geochemistry*, v. 172, pp. 106105, 2024. doi: https://doi.org/10.1016/j.apgeochem.2024.106105.

[12] SINGH, P.K., LOGESH, K., KUMAR, S.S., *et al.*, "Revolutionizing the material performance of AZ64/ZrB2 composites for engineering applications", *Matéria*, v. 30, pp. e20240356, 2025. doi: https://doi.org/10.1590/1517-7076-rmat-2024-0356.

[13] SONGA, H.K., SUMAN, K.N.S., MANYALA, A.R., "FE simulation of uniaxial tensile behavior of SiC reinforced AA5083 alloy", *Matéria*, v. 29, n. 1, pp. e20230173, 2024. doi: https://doi.org/10.1590/1517-7076-rmat-2023-0173.

[14] KUPPUSAMY, R., THANGAVEL, A., MANICKAM, A., *et al.*, "The influence of MoS 2 and SiC reinforcement on enhancing the tribological and hardness of aluminium matrix (Al6061-T6) hybrid composites using Taguchi's method", *Matéria*, v. 29, n. 1, pp. e20230337, 2024. doi: https://doi.org/10.1590/1517-7076-rmat-2023-0337.

[15] INEGBENEBOR, A.O., BOLU, C.A., BABALOLA, P.O., *et al.*, "Aluminum silicon carbide particulate metal matrix composite development via stir casting processing", *Silicon*, v. 10, n. 2, pp. 343–347, 2018. doi: https://doi.org/10.1007/s12633-016-9451-7.

[16] TENALI, N., GANESAN, G., RAVINDRA BABU, P., "Corrigendum: A study on the effects of hybrid (SIC- PSSA) nano sized reinforcement on mechanical and tribological behaviour of Al alloy-based metal matrix composite produced by ultrasonic assisted stir casting", *Materials Research Express*, v. 11, n. 7, pp. 119501, 2024. doi: https://doi.org/10.1088/2053-1591/ad8873.

[17] ANAND, A., TIWARI, S.K., "Recent advancements in the production of hybrid metal matrix composites (HMMC): a review", *IOP Conference Series. Materials Science and Engineering*, v. 1248, n. 1, pp. 12087, 2022. doi: https://doi.org/10.1088/1757-899X/1248/1/012087.

[18] SOUNDARARAJAN, R., SIVASANKARAN, S., AL-MUFADI, F.A., *et al.*, "Investigation on A356-20wt%SiC composites through mechanical stirring and ultra-sonic-assisted cavitation", *Materials Research Express*, v. 6, n. 9, pp. 96572, 2019. doi: https://doi.org/10.1088/2053-1591/ab3082.

[19] KHALID, M.Y., UMER, R., KHAN, K.A., "Review of recent trends and developments in aluminium 7075 alloy and its metal matrix composites (MMCs) for aircraft applications", *Results in Engineering*, v. 20, pp. 101372, 2023. doi: https://doi.org/10.1016/j.rineng.2023.101372.

[20] CHANNAR, H.R., ULLAH, B., NASEEM, M.S., *et al.*, "Mechanical properties and microstructural investigation of AA2024-T6 reinforced with Al2O3 and SiC metal matrix composites", *Eng*, v. 5, n. 4, pp. 3023–3032, 2024. doi: https://doi.org/10.3390/eng5040157.

[21] SATHISHKUMAR, A., SOUNDARARAJAN, R., RAMESH, A., *et al.*, "Experimental investigations on Mechanical and Tribological behaviour of A356 with x wt% boron carbide and fly ash hybrid compositeS", *IOP Conference Series. Materials Science and Engineering*, v. 988, n. 1, pp. 12023, 2020. doi: https://doi.org/10.1088/1757-899X/988/1/012023.

[22] BABU, N., SOUNDARARAJAN, R., SANTHOSH, V.J., *et al.*, "Effect of processing route on the mechanical and tribological behaviour of AA8011 hybrid composites", *Journal of The Institution of Engineers (India): Series D*, v. 104, n. 2, pp. 561–567, 2023. doi: https://doi.org/10.1007/s40033-022-00407-0.

[23] NURUZZAMAN, D.M., KAMARUZAMAN, F.F.B., "Processing and mechanical properties of aluminium-silicon carbide metal matrix composites", *IOP Conference Series. Materials Science and Engineering*, v. 114, pp. 012123, 2016. doi: https://doi.org/10.1088/1757-899X/114/1/012123.

[24] SIDDHARTHAN, B., RAJIEV, R., SARAVANAN, S., *et al.*, "Effect of silicon carbide in mechanical properties of aluminium alloy based metal matrix composites", *IOP Conference Series. Materials Science and Engineering*, v. 764, n. 1, pp. 012040, 2020. doi: https://doi.org/10.1088/1757-899X/764/1/012040.

[25] BONTHALA, S.R., VELLINGIRI, S., SRIDHAR, V.P., *et al.*, "Mechanical and wear optimization investigation of Titanium alloy nanocomposites made with selective laser melting process", *Matéria*, v. 30, pp. e20240718, 2025. doi: https://doi.org/10.1590/1517-7076-rmat-2024-0718.

[26] SENTHIL KUMAR, M., VANMATHI, M., SAKTHIVEL, G., "SiC Reinforcement in the Synthesis and Characterization of A356/AL2O3/Sic/Gr Reinforced Composite-Paving a Way for the Next Generation of Aircraft Applications," *Silicon,* v. 13, n. 8, pp. 2737–2744, 2020. doi: https://doi.org/10.1007/S12633-020-00625-9

[27] KUMAR, D., ANGRA, S., SINGH, S., "Mechanical Properties and Wear Behaviour of Stir Cast Aluminum Metal Matrix Composite: A Review," *International Journal of Engineering*, v. 35, pp. 794–801, 2022. doi: https://doi.org/10.5829/ije.2022.35.04a.19

[28] BELDAR, P., KUMAVAT, H.R., "Comparative analysis of mechanical properties of SiC particle addition on Al6061/Ni and Al6061/Cr metal matrix composites," *Mater Lett*., v. 369, pp. 136745, 2024. doi: https://doi.org/10.1016/J.MATLET.2024.136745

[29] RUMI, M.J.U., SARKER, A.A., MALIYAT, N., et al., "Fabrication of aluminium metal matrix composites with Al 6063 reinforced with Al2O3 by two step stir casting method for investigation of mechanical properties," *International Journal of Microstructure and Materials Properties,* v. 17, pp. 267–279, 2024. doi: https://doi.org/10.1504/IJMMP.2024.137984

[30] RABIEI, A., ENOKI, M., KISHI, T., "Study on fracture behavior of particle reinforced metal matrix composites by using acoustic emission source characterization", *Materials Science and Engineering A*, v. 293, n. 1–2, pp. 81–87, 2000. doi: https://doi.org/10.1016/S0921-5093(00)01218-1.

[31] GRASSI, G.D., SCHNEIDER, E.L., OLIVEIRA, C.T., *et al.*, "Evaluation of the use of Al-Mg-Sc system alloys for wings spars in the aerospace sector", *Matéria*, v. 30, pp. e20240706, 2025. doi: https://doi.org/10.1590/1517-7076-rmat-2024-0706.

[32] YU, Y.H., CHOI, J.H., KWEON, J.H., *et al.*, "A study on the failure detection of composite materials using an acoustic emission", *Composite Structures*, v. 75, n. 1–4, pp. 163–169, 2006. doi: https://doi.org/10.1016/j.compstruct.2006.04.070.

[33] CHOUDHURY, A., NANDA, J., DAS, S.N., "Sintering sensitivity of aluminium metal matrix composites developed through powder metallurgy proposed technique-a review", *Journal of Physics: Conference Series*, v. 2070, n. 1, pp. 12193, 2021. doi: https://doi.org/10.1088/1742-6596/2070/1/012193.

[34] STEPANOVA, L., RAMAZANOV, I., CHERNOVA, V., "Acoustic and emission analysis of the defect nucleation process in carbon fiber reinforced plastic samples", *Transportation Research Procedia*, v. 54, pp. 320–327, 2021. doi: https://doi.org/10.1016/j.trpro.2021.02.078.

[35] MUSSATTO, A., AHAD, I., MOUSAVIAN, R., *et al.*, "Advanced production routes for metal matrix composites", *Engineering Reports*, v. 3, n. 5, pp. e12330, 2020. doi: https://doi.org/10.1002/eng2.12330.

[36] RAJAN, T.P.D., PILLAI, R.M., PAI, B.C., "Characterization of centrifugal cast functionally graded aluminum-silicon carbide metal matrix composites", *Materials Characterization*, v. 61, n. 10, pp. 923–928, 2010. doi: https://doi.org/10.1016/j.matchar.2010.06.002.

[37] AGRAWAL, M., SINGH, S., "Cold forging of silicon carbide particulate (SiCp) reinforced aluminium metal matrix composite preforms", *IOP Conference Series. Materials Science and Engineering*, v. 1045, n. 1, pp. 12026, 2021. doi: https://doi.org/10.1088/1757-899X/1045/1/012026.

[38] SENTHILNATHAN, T., BALACHANDAR, K., "Mechanical and microstructure evaluation of novel hybrid TiB2/B4C aluminium metal matrix composite", *Materials Research Express*, v. 10, n. 6, pp. 66509, 2023. doi: https://doi.org/10.1088/2053-1591/acda18.

[39] SIJO, M.T., JAYADEVAN, K.R., "Characterization of stir cast aluminium silicon carbide metal matrix composite", *Materials Today: Proceedings*, v. 5, n. 11, pp. 23844–23852, 2018. doi: https://doi.org/10.1016/j.matpr.2018.10.176.

[40] PAWAR, P.B., UTPAT, A.A., "Development of aluminium based silicon carbide particulate metal matrix composite for spur gear", *Procedia Materials Science*, v. 6, pp. 1150–1156, 2014. doi: https://doi.org/10.1016/j.mspro.2014.07.187.

[41] BARADESWARAN, A., ELAYAPERUMAL, A., "Influence of B4C on the tribological and mechanical properties of Al 7075–B4C composites", *Composites. Part B, Engineering*, v. 54, pp. 146–152, 2013. doi: https://doi.org/10.1016/j.compositesb.2013.05.012.

[42] LIN, J.T., BHATTACHARYYA, D., LANE, C., "Corrigendum to "Machinability of a silicon carbide reinforced aluminium metal matrix" [Wear 181–183 (1995) 883–888] (PII:0043-1648(94)07109-8)", *Wear*, v. 189, pp. 144, 1995. doi: https://doi.org/10.1016/0043-1648(95)06720-5.

[43] KALYAN CHARAN, A., UDAY KUMAR, R., BALUNAIK, B., "Evaluation of convective heat transfer coefficient and heat transfer rate through aluminium metal matrix composite fin made by stir casting", *IOP Conference Series. Materials Science and Engineering*, v. 1057, pp. 12038, 2021. doi: https://doi.org/10.1088/1757-899X/1057/1/012038.

[44] SIJO, M.T., JAYADEVAN, K.R., "Analysis of stir cast aluminium silicon carbide metal matrix composite: a comprehensive review", *Procedia Technology*, v. 24, pp. 379–385, 2016. doi: https://doi.org/10.1016/j.protcy.2016.05.052.

[45] MHASKE, M.S., SHIRSAT, U.M., "An investigation of mechanical properties of aluminium based silicon carbide (AlSiC) metal matrix composite by different manufacturing methods", *Materials Today: Proceedings*, v. 44, pp. 376–382, 2021. doi: https://doi.org/10.1016/j.matpr.2020.09.746.

[46] SHARMA, A.K., BHANDARI, R., PINCA-BRETOTEAN, C., "Impact of silicon carbide reinforcement on characteristics of aluminium metal matrix composite", *Journal of Physics: Conference Series*, v. 1781, n. 1, pp. 012031, 2021. doi: https://doi.org/10.1088/1742-6596/1781/1/012031.

[47] SHALINI KORA, P.L.S., GORANTLA, N., "Study on behaviour of aluminium metal matrix composite reinforced with silicon carbide and titanium diboride", *IOP Conference Series. Earth and Environmental Science*, v. 1130, n. 1, pp. 12030, 2023. doi: https://doi.org/10.1088/1755-1315/1130/1/012030.

[48] KOK, M., "Production and mechanical properties of Al2O3 particle-reinforced 2024 aluminium alloy composites", *Journal of Materials Processing Technology*, v. 161, n. 3, pp. 381–387, 2005. doi: https://doi.org/10.1016/j.jmatprotec.2004.07.068.

[49] REDDY, P.S., KESAVAN, R., VIJAYA RAMNATH, B., "Investigation of mechanical properties of Aluminium 6061-silicon carbide, boron carbide metal matrix composite", *Silicon*, v. 10, n. 2, pp. 495–502, 2018. doi: https://doi.org/10.1007/s12633-016-9479-8.

[50] JEYKRISHNAN, J., VIJAYA RAMNATH, B., HERVIN SAVARIRAJ, X., *et al.*, "Investigation on tensile and impact behavior of aluminum base silicon carbide metal matrix composites", *Indian Journal of Science and Technology*, v. 9, n. 37, pp. 2–5, 2016. doi: https://doi.org/10.17485/ijst/2016/v9i37/101979.

[51] RAM KUMAR, S., RAMAKRISHNAN, S., RISVAK, M., *et al.*, "Experimental analysis and characterization of Mechanical, Physical properties of Aluminium (Al6061) Metal Matrix composite reinforced with SiC and Al2O3 using Stir casting", *IOP Conference Series. Materials Science and Engineering*, v. 1145, n. 1, pp. 12109, 2021. doi: https://doi.org/10.1088/1757-899X/1145/1/012109.

[52] CHANDRADASS, J., THIRUGNANASAMBANDHAM, T., JAWAHAR, P., *et al.*, "Effect of silicon carbide and silicon carbide/alumina reinforced aluminum alloy (AA6061) metal matrix composite", *Materials Today: Proceedings*, v. 45, pp. 7147–7150, 2020. doi: https://doi.org/10.1016/j.matpr.2021.02.143.

[53] DEBNATH, S., ROY, S., KUMAR PRAMANICK, A., "An exploratory comparative study of fabricated silica – aluminium metal matrix composites with casted aluminium-silicon alloys", *Journal of Physics: Conference Series*, v. 1579, n. 1, pp. 12014, 2020. doi: https://doi.org/10.1088/1742-6596/1579/1/012014.

[54] SIDDHARTHAN, B., RAJIEV, R., SARAVANAN, S., *et al.*, "Effect of silicon carbide in mechanical properties of aluminium alloy based metal matrix composites ", *IOP Conference Series. Materials Science and Engineering*, v. 764, n. 1, pp. 012040, 2020. doi: https://doi.org/10.1088/1757-899X/764/1/012040.

[55] KHAIREEZ, M.H.M., YUSUF, N.K., GHALEB, A.M., *et al.*, "Life cycle assessment of direct recycling hot press forging of aluminium AA7075 metal matrix composite", *Materials Research Express*, v. 11, n. 3, pp. 36519, 2024. doi: https://doi.org/10.1088/2053-1591/ad3011.

[56] SHETTY, S., SHETTY, R., SHETTY, N., *et al.*, "An integrated experimental and analytical approach on mechanical characterization of advanced powder metallurgy aluminium metal matrix composites reinforced with different particulates", *Materials Research Express*, v. 11, n. 5, pp. 56515, 2024. doi: https://doi.org/10.1088/2053-1591/ad4aef.

[57] MANIKONDA, R.D., KOSARAJU, S., RAJ, K.A., *et al.*, "Wear behavior analysis of silica carbide based aluminum metal matrix composites", *Materials Today: Proceedings*, v. 5, n. 9, pp. 20104–20109, 2018. doi: https://doi.org/10.1016/j.matpr.2018.06.377.

[58] SHETTY, S., SHETTY, R., SHETTY, N., *et al.*, "An integrated experimental and analytical approach on mechanical characterization of advanced powder metallurgy aluminium metal matrix composites reinforced with different particulates", *Materials Research Express*, v. 11, n. 5, pp. 56515, 2024. doi: https://doi.org/10.1088/2053-1591/ad4aef.

[59] MOMON, S., MOEVUS, M., GODIN, N., *et al.*, "Acoustic emission and lifetime prediction during static fatigue tests on ceramic-matrix-composite at high temperature under air", *Composites. Part A, Applied Science and Manufacturing*, v. 41, n. 7, pp. 913–918, 2010. doi: https://doi.org/10.1016/j.compositesa.2010.03.008.

[60] EL MOHTADI, R., RZECZKOWSKI, J., KORZEC-STRZAŁKA, I., *et al.*, "Experimental tensile testing of the lap joint composite laminates supported with the acoustic emission and machine learning techniques", *Composite Structures*, v. 345, pp. 118394, 2024. doi: https://doi.org/10.1016/j.compstruct.2024.118394.

[61] RISHIKESAN, V., CHATURVEDI, B., ARUNACHALAM, N., "Characterisation of drilling-induced damage in GFRP honeycomb sandwich composites using acoustic emission", *Procedia Manufacturing*, v. 53, pp. 664–672, 2021. doi: https://doi.org/10.1016/j.promfg.2021.06.066.

[62] SELVARAJ, V.K., SUBRAMANIAN, J., SUYAMBULINGAM, I., *et al.*, "Influence of bio-based kenaf polymer composites on mechanical and acoustic properties for futuristic applications: An initiative towards net-zero carbon emissions", *Polymer Testing*, v. 134, pp. 108409, 2024. doi: https://doi.org/10.1016/j.polymertesting.2024.108409.

[63] BÜYÜKÖZTÜRK, O., TAŞDEMIR, M.A., GÜNEŞ, O., *et al.*, *Nondestructive Testing of Materials and Structures: Proceedings of NDTMS-2011, Istanbul, Turkey, May 15-18, 2011*, RILEM Bookseries 6, Dordrecht, Springer Dordrecht, 2012. doi: https://doi.org/10.1007/978-94-007-0723-8.

[64] MUMMERY, P.M., DERBY, B., SCRUBY, C.B., "Acoustic emission from particulate-reinforced metal matrix composites", *Acta Metallurgica et Materialia*, v. 41, n. 5, pp. 1431–1445, 1993. doi: https://doi.org/10.1016/0956-7151(93)90252-N.

[65] THIRUKKUMARAN, K., MUKHOPADHYAY, C.K., "Analysis of acoustic emission signal to characterization the damage mechanism during drilling of Al-5%SiC metal matrix composite", *Silicon*, v. 13, n. 2, pp. 309–325, 2021. doi: https://doi.org/10.1007/s12633-020-00426-0.

[66] VIO, P., KAPLAN, A., GOMEZ, M.P., *et al.*, "Characterization of metal/ceramic interfaces in dental materials by acoustic emission", *Procedia Materials Science*, v. 8, pp. 683-692, 2015. doi: https://doi.org/10.1016/j.mspro.2015.04.125.

[67] KONG, X., WANG, Y.M., ZHANG, X., *et al.*, "Monitoring damage evolution in a titanium matrix composite shaft under torsion loading using acoustic emission", *Acta Metallurgica Sinica*, v. 32, n. 10, pp. 1244–1252, 2019. doi: https://doi.org/10.1007/s40195-019-00888-1.

[68] RABIEI, A., ENOKI, M., KISHI, T., "A study on fracture behavior of particle reinforced metal matrix composites by using acoustic emission source characterization", *Materials Science and Engineering A*, v. 293, n. 1–2, pp. 81–87, 2000. doi: https://doi.org/10.1016/S0921-5093(00)01218-1.

[69] YANG, Y., LAN, J., LI, X., "Study on bulk aluminum matrix nano-composite fabricated by ultrasonic dispersion of nano-sized SiC particles in molten aluminum alloy", *Materials Science and Engineering A*, v. 380, n. 1–2, pp. 378–383, 2004. doi: https://doi.org/10.1016/j.msea.2004.03.073.

[70] THIRUKKUMARAN, K., MUKHOPADHYAY, C.K., "Acoustic emission signals analysis to differentiate the damage mechanism in the drilling of Al-5%B4C metal matrix composite", *Ultrasonics*, v. 124, pp. 106762, 2022. doi: https://doi.org/10.1016/j.ultras.2022.106762. PubMed PMID: 35644099.

[71] THIRUKKUMARAN, K., MUKHOPADHYAY, C.K., "Analysis of acoustic emission signal to characterization the damage mechanism during drilling of Al-5%SiC metal matrix composite", *Silicon*, v. 13, n. 2, pp. 309–325, 2021. doi: https://doi.org/10.1007/s12633-020-00426-0.

[72] VANNIAMPARAMBIL, P.A., GUCLU, U., KONTSOS, A., "Identification of crack initiation in aluminum alloys using acoustic emission", *Experimental Mechanics*, v. 55, n. 5, pp. 837–850, 2015. doi: https://doi.org/10.1007/s11340-015-9984-5.

[73] HENNEKE 2ND, E.G., HERAKOVICH, C.T., JONES, G.L., *et al.*, "Acoustic emission from composite-reinforced metals", *Experimental Mechanics*, v. 15, n. 1, pp. 10–16, 1975. doi: https://doi.org/10.1007/BF02318519.

DATA AVAILABILITY

The data that support the findings of this study are available on request from the corresponding author. The data are not publicly available due to privacy or ethical restrictions.